Prefrontal Mechanisms of Fear Reduction After Threat Offset

Floris Klumpers, Mathijs A.H.L. Raemaekers, Amber N.V. Ruigrok, Erno J. Hermans, J. Leon Kenemans, and Johanna M.P. Baas

Introduction: Reducing fear when a threat has disappeared protects against a continuously elevated anxiety state. In this study, we investigated the brain mechanism involved in this process.

Methods: The threat paradigm consisted of discrete cues that signaled either threat of shock or safety. Healthy participants were tested in two sessions in which eyeblink startle ($n = 26$) and blood oxygen level dependence ($n = 23$) were measured to index subjects' defensive state and brain responses respectively.

Results: Startle results indicated that subjects could rapidly decrease their defensive state after the offset of shock threat. Functional magnetic resonance imaging data indicated that the termination of threat was associated with the recruitment of lateral and ventromedial prefrontal cortices. An exploratory connectivity analysis showed that activity in these prefrontal regions was linked and was also associated with activity in brain regions typically responding to threat, the right anterior insula and amygdala.

Conclusions: These results provide first evidence for a prefrontal mechanism that functions to control anxiety after threat offset, which may be dysfunctional in patients who suffer from excessive sustained anxiety. Moreover, the results support a model in which the lateral prefrontal cortex controls anxiety related limbic activity through connections with ventromedial prefrontal cortex.

Key Words: Anxiety, emotion regulation, fear, fMRI, imaging, prefrontal cortex, startle

When facing threat, the brain rapidly engages the neuroanatomic systems that support an adaptive response. Under normal circumstances, when danger is no longer perceived to be imminent, these systems are switched off to prevent unnecessary energy expenditure and negative side effects of prolonged stress. However, a sustained state of anxiety may emerge in individuals who fail to reduce fear adaptively after a threat signal has disappeared. To investigate the neural systems involved in this control process, this study explored neural correlates of the transition from a threatening situation to a resting phase using functional magnetic resonance imaging (fMRI).

It is widely acknowledged that deficits in neurobiological mechanisms of fear reduction may play an important role in some forms of anxiety disorders (1,2). Excessive sustained anxiety appears to be a hallmark of some disorders of anxiety—for example, generalized anxiety disorder (3,4). However, many previous studies on fear regulation have focused on control mechanisms operating during presentation of discrete threatening stimuli (5–7) and have not investigated the brain's natural control mechanisms that terminate the anxious state in the period following threat offset (7).

Previous neuroimaging studies that have investigated the neural substrate of top-down fear modulation have consistently found evidence for involvement of the prefrontal cortex (PFC) (5,8) in this process. Extinction of a conditioned fear response, an increasingly well-investigated fear inhibition paradigm, is associated with activity changes in ventromedial PFC regions (9,10). In addition, neuroimaging research with cognitive appraisal paradigms has shown that areas of dorsolateral PFC are being recruited during more deliberate emotional regulation (11–13). Given the relative lack of connections between the limbic system and dorsolateral PFC (14,15), the PFC may inhibit fear through connections of the ventromedial PFC with the amygdala in both forms of fear regulation (16). We hypothesized that the PFC may orchestrate reductions in fear that occur after the offset of a danger cue in a manner similar to the effects observed during fear extinction and cognitive regulation. In this way, the PFC may play an important role in the control of sustained anxiety.

To study brain areas associated with threat offset, subjects were presented with a cue signaling threat of receiving an electric shock, and another stimulus that indicated safety from shock. Fear was indexed in a session separate from the fMRI by measuring potentiation of the startle reflex, an objective and robust method for measuring defensive states in humans (17–19). Startle probes were presented at different time points after threat onset and offset to capture the time course of the defensive response (20–25). This also yielded a valid assessment of fear levels during the fMRI session, because fear-potentiated startle remains at similar levels across repeated tests in our instructed fear paradigm (26). Specifically, we tested the hypotheses that the offset of threatening stimuli is associated with 1) a significant reduction in fear indexed by startle amplitude and 2) with concurrent ventromedial and lateral PFC activation.

Methods and Materials

Subjects

Subjects included 26 healthy participants aged 18–30 (mean 22.1 years) who gave written informed consent before participation. Three subjects were not scanned because of technical issues with the MRI scanner after already participating in the startle session. The final sample therefore consisted of 23 subjects (11 female) for the imaging data and 26 (12 female) for the startle session.

From the Departments of Experimental Psychology (FK, MAHLR, ANVR, JLK, JMPB) and Psychopharmacology (FK, JLK, JMPB), Utrecht University, Utrecht, the Netherlands; Donders Institute for Brain, Cognition and Behaviour (EJH) and Department of Neurology (EJH), Radboud University Nijmegen Medical Centre, Nijmegen, the Netherlands.

Address correspondence to Floris Klumpers, Msc., Department of Experimental Psychology, 3508 TC Utrecht, the Netherlands; E-mail: F.Klumpers@uu.nl.

Received Mar 13, 2010; revised Aug 31, 2010; accepted Sep 1, 2010.

0006-3223/$36.00
doi:10.1016/j.biopsych.2010.09.006

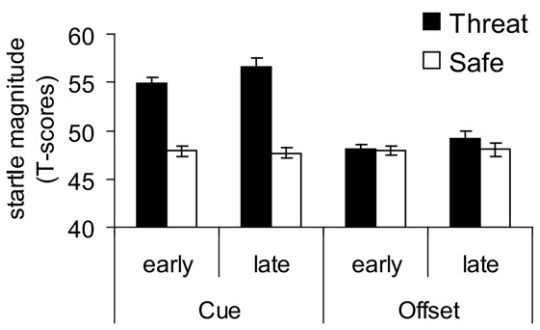

Figure 1. Mean startle magnitude during the threat and safe cues and after cue offset. Early probes were presented 1.5 to 3.5 sec after cue onset or offset and late cues after 5.5–11.5 sec. Error bars represent standard error of the mean.

Procedure and Task

During a screening visit, subjects filled in a battery of personality and medical questionnaires and underwent a shock workup procedure (described more in Supplement 1) to set the shock intensity individually for the first session. After subjects had been admitted to the study, they were invited for two sessions separated by 2 to 14 days. We randomly assigned subjects to participate first in either the fMRI (n = 12) or startle (n = 14) session. The experimental paradigm for both sessions was identical. Before each session, subjects again underwent a shock workup procedure to reset the shock intensity. After the workup, instructions consisted of the sequential presentation of two pictures of faces with on-screen instructions that subjects could receive shocks at any time during presentation of Picture 1 and never during Picture 2. Pictures were photos of two male faces selected from the Psychological Image Collection at Stirling (http://pics.psych.stir.ac.uk) that each received neutral ratings in a pilot study. One of the pictures was presented in blue and the other in yellow to increase salience and distinctiveness of the cues. Association between the pictures and either threat or safety was counterbalanced across subjects. The subjects were explicitly instructed to rest when there was no face on the screen. Accordingly, the word *RUST* ("rest" in Dutch) was presented on the screen during the intertrial interval.

The experiment consisted of three 10-min runs that contained 14 presentations of each face. Pictures were presented in a semi-random order, counterbalanced over subjects and sessions, with no more than three consecutive repetitions of the same condition. Picture duration varied between 6 and 12 sec (9.3 sec average). The rest period between pictures ranged between 8 and 12 sec (9.9 sec average). Shocks were presented at varying time points during the threat condition. Two or three shocks were administered per run, with a total of six shocks for the first session and seven shocks for the second session. After each run, subjects retrospectively rated their anxiety during and immediately after the offset of the threat and safe cues on a scale from 0 (*not anxious/nervous*) to 10 (*very anxious/nervous*).

Electromyographic recording of the eyeblink startle reflex, startle probe presentation, and shock administration were carried out using previously published procedures (26). Briefly, startle probes were 50-msec, 106-dB(A) white-noise bursts, and the eyeblink startle reflex was measured from the orbicularis oculi with two Ag-AgCl electrodes placed under the right eye during the startle session. In the startle session, startle probes could be presented either between 1.5 and 3.5 sec following picture onset (early probes) or 5.5 to 11.5 sec post-onset (late probes). Similarly, probes were also presented either 1.5 to 3.5 or 5.5 to 11.5 sec after the offset of the threat and safe cues. For each condition, three probes were presented per run at each latency summing to a total of 72 (three runs $\times$ two conditions $\times$ four probe latencies $\times$ three) probes. The mean interval between probes was 21.6 sec, with a minimum interval of 14 sec after a shock reinforcement or previous probe. To avoid distortion of the magnetic resonance signal by shock stimulation, a nonmagnetic high-pass filter was placed between the stimulator and the MRI-compatible, carbon-wired silver electrodes used for shock administration. The same filter and electrodes were also used during the startle session to keep the shock intensity comparable. The intensity of the electrical stimulation varied between subjects and over sessions from .7 to 7.6 mA.

Imaging

Imaging was performed on a Philips 3T Achieva MRI scanner (Philips Medical Systems, Best, the Netherlands), 2250 T2*-weighted volumes of .813 sec obtained in three runs (echo time = 23 msec, repetition time = 15.6 msec, field of view = 224 $\times$ 224 $\times$ 136.5 mm, flip angle = 8.85°, matrix = 64 $\times$ 64, voxel size = 3.5 mm isotropic). Each volume consisted of 39 sagittal slices. The 3D PRESTO sequence (27,28) was used combined with echo shifting and parallel imaging acceleration (29), which allows fast whole brain scanning (27). Furthermore, we used in-plane segmentation (30), allowing a shorter echo-train length and lower echo time to reduce distortion artefacts and to reduce signal dropout in regions

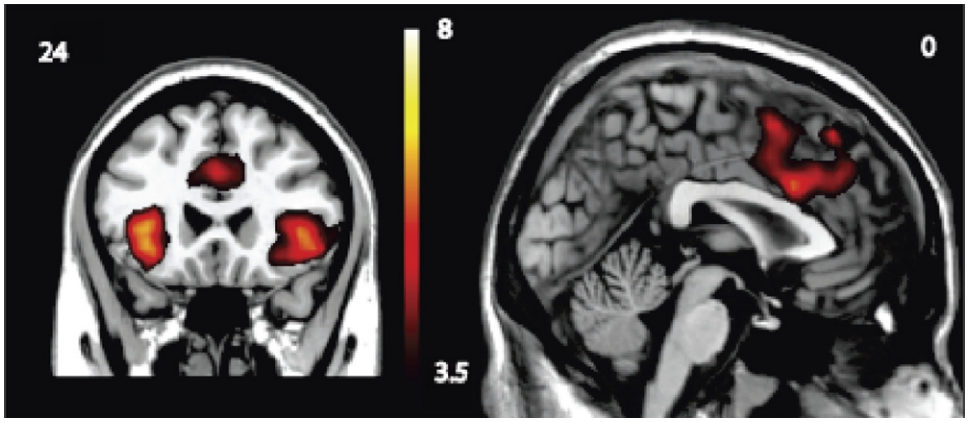

Figure 2. Functional magnetic resonance group results for the threat versus safe (sustained) contrast showing activations in bilateral insula/inferior frontal gyrus and anterior cingulate cortex during threat. Results are visualized on an anatomic template image; and the number in the top right corner represents the Montreal Neurological Institute coordinate for the selected slice, and the scale is in t scores.

Table 1. Functional Magnetic Resonance Imaging Group Results

Region (of Peak Activation)	Montreal Neurological Institute Coordinates			*z* Score	Voxels
	X	*Y*	*Z*		
Threat > Safe[a]					
Right anterior insula/ inferior frontal gyrus	49	21	−7	4.97	273
Left anterior insula/ inferior frontal gyrus	−35	21	−7	4.96	291
Posterior cingulate gyrus	4	−24	28	4.93	65
Anterior cingulate gyrus	0	18	28	4.71	463
Right supramarginal gyrus	49	−42	32	4.65	209
Right medial frontal gyrus	46	4	42	4.51	67
Right thalamus	7	−14	10	4.32	187
Cerebellum	0	−56	−24	4.29	145
Left cerebellum	−38	−60	−32	4.15	153
Right medial frontal gyrus	46	38	32	4.09	144
Left lingual gyrus	−21	−102	−14	3.77	54
Left middle frontal gyrus	−46	49	21	3.54	53
Left supramarginal gyrus	−56	−49	26	3.46	46
Safe > Threat[a]					
Right superior parietal lobule	24	−66	60	5.22	62
Left precuneus	−35	−88	35	5.22	233
Medial frontal gyrus	0	60	−14	5.19	99
Precuneus	0	−56	38	4.91	452
Right postcentral gyrus	66	−18	38	4.39	102
Right parahippocampal gyrus	18	−14	24	4.37	74
Left parahippocampal gyrus	−21	−21	−18	4.30	52
Left superior frontal gyrus	−28	21	56	4.28	54
Right superior occipital gyrus	42	−88	28	4.14	130
Left postcentral gyrus	−63	−18	49	4.09	70
Left postcentral gyrus	−32	−35	77	3.95	64
Threat Offset > Safe Offset[b]					
Right middle frontal gyrus (lateral prefrontal cortex)	35	66	4	4.11	53
Safe offset > threat offset[b]					
Medial frontal gyrus (subgenual ventromedial prefrontal cortex)	0	35	−14	3.59	42

[a]Statistical images assessed for cluster-wise significance; with a cluster defining threshold of $p = .001$, uncorrected, the .05 family wise error–corrected critical cluster size was 38 voxels.

[b]Statistical images assessed for cluster-wise significance; with a cluster-defining threshold of $p = .001$, uncorrected, the .05 FWE-corrected critical cluster size was 37 voxels.

susceptible for artefacts (e.g., ventral prefrontal areas, amygdalae). After the functional runs, a T1-weighted anatomic image of 175 sagittal slices was obtained (echo time = 3.8 msec, repetition time = 8.4 msec, field of view = 288 × 288 × 175 mm, flip angle = 17°, voxel size = 1 mm isotropic).

Data Processing and Analysis

Startle data were preprocessed and checked for artifacts according to previously published procedures and guidelines (26,31,32), described in more detail in Supplement 1. Startle magnitudes were transformed to *t* scores per subject, and trials were averaged according to condition and probe time (threat/safe, onset/offset, early/late). Statistical analyses for the startle data and subjective anxiety ratings consisted of repeated-measures analyses of variance (ANOVA) carried out in SPSS 16 (SPSS, Chicago, Illinois). For the anxiety ratings, threat condition (threat, safe) and time (cue, offset) were entered as within subjects factors. For the startle data, probe latency (early, late) was also included to create a four-level latency factor (cue early, cue late, offset early, offset late). A between subjects factor "order" was added to verify that there was no influence of previous exposure to the task.

The fMRI data were processed using SPM5 (Welcome Department of Imaging Neuroscience, University College London, United Kingdom; http://www.fil.ion.ucl.ac.uk/spm/). Functional scans were realigned, coregistered to the anatomic scan, and spatially normalized to the Montreal Neurological Institute T1 template image to a normalized resolution of 3.5 mm isotropic. The normalized images were then smoothed with a kernel with a full width at half maximum of 8 × 8 × 8 mm. Subsequently a general linear model was composed to relate blood oxygen level–dependent (BOLD) signal variation to the task conditions. The predictors in this model were the threat conditions, safe conditions, and shocks. For the threat and safe conditions, the onset and offset responses were modeled using a delta function. In addition, a sustained response to the cues was modeled with a boxcar that lasted throughout the threat and safe conditions. These regressors were convolved with the canonical hemodynamic response function. Multiple correlations between factors in the design were calculated to assess multicollinearity. All were around .40. Realignment parameters were included in the model to reduce movement-related artefacts. Visual inspection of the scans around shock administration indicated extremely large and fast signal fluctuations. Therefore, each scan that contained these excessive fluctuations was modeled using a separate regressor. In this way, we removed any variance caused by these artifacts that could reduce statistical power for detecting our effects of interest. This was the case for 11 subjects, with, on average, around seven scans per subject removed because of artifacts.

One-sample *t* tests were used to test for significant group effects for the contrasts comparing the threat and safe condition and their offsets. For the assessment of the impact of the threat cues, we only report the results from the sustained contrasts here; the results that compared threat and safe onset overlapped and did not give any additional activation in our areas of interest. Results were thresholded at $p < .001$ (uncorrected for multiple comparisons). To minimize the chance of false positives, this voxelwise threshold was combined with a cluster threshold, and only clusters that survived a threshold of .05 (family-wise error corrected using random field theory) are reported.

Because of our a priori expectations on activations in limbic areas and prefrontal areas, we selected the clusters of activity in the insula and anterior cingulate cortex (ACC; threat vs. safe sustained contrast) (1,33–38) and prefrontal areas (offset contrast) (5,6,10–12,16) for further analyses on the basis of the whole-brain analyses. Mean signal change, relative to the mean signal in the cluster, was extracted from these areas using the MARSBAR toolbox (39) in SPM. Besides these functional regions of interest (ROIs), we also included the amygdala as an anatomic ROI because of extensive evidence for a role of the amygdala in fear. To this end, we extracted the average signal change from the bilateral amygdalae using an anatomic mask from the automated anatomical labeling atlas (40). Between-subjects correlations were then calculated between mean signal change in our ROIs and startle potentiation. All correlations reported remained significant

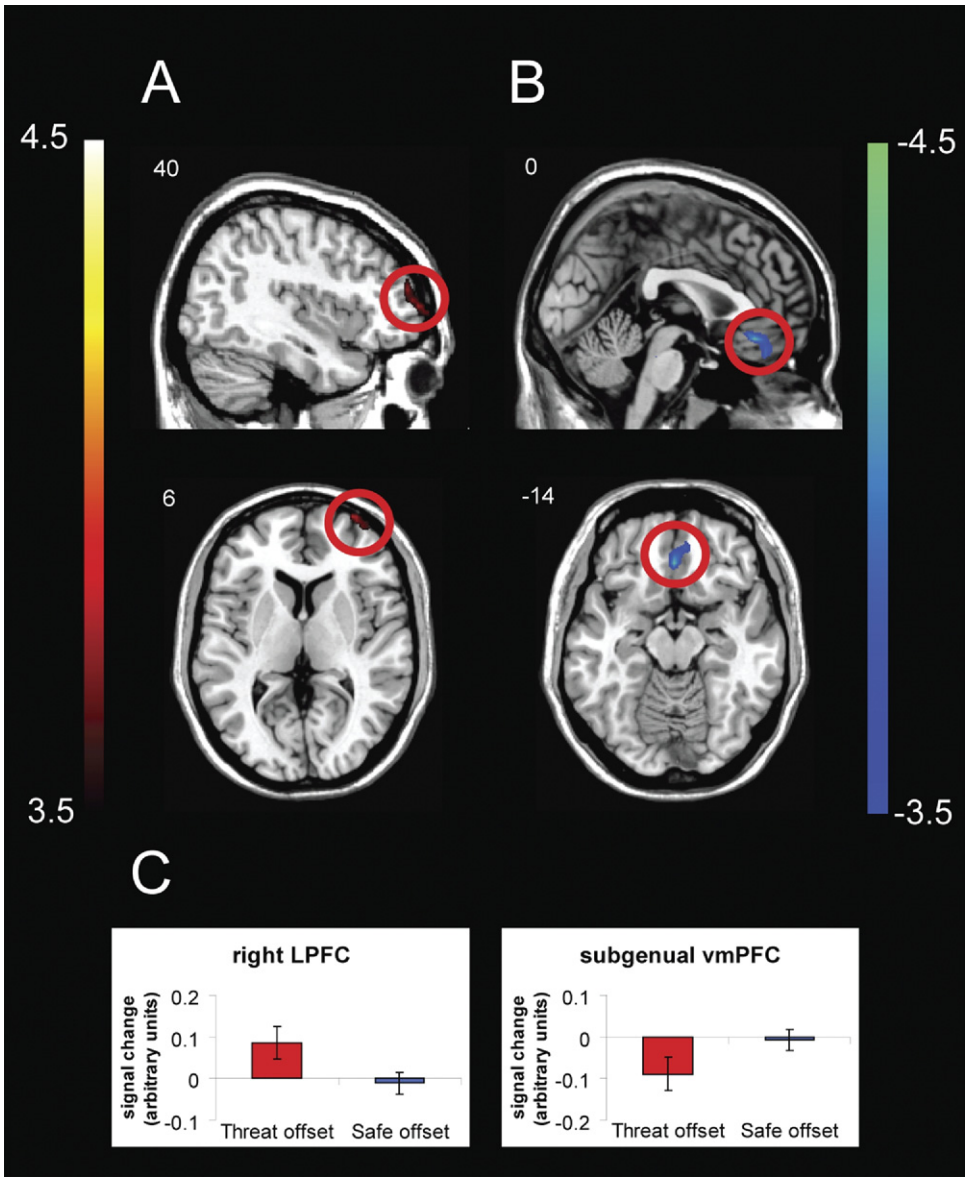

Figure 3. Functional magnetic resonance group results for the threat versus safe offset contrast. **(A)** Loci of activation in the lateral prefrontal cortex (LPFC) and **(B)** deactivation in the subgenual ventromedial PFC (vm)PFC in reaction to threat offset. Results are visualized on an anatomic template image; the number in the top right corner represents the Montreal Neurological Institute coordinate for the selected slice, and the scale is in *t* scores. **(C)** Mean percent signal change for each regions of interest for the threat and safe conditions separately, error bars represent standard error of the mean.

when removing outlier data points with absolute *z* scores > 2.5 (*z* scores calculated over subjects for each variable). To visualize the individual contribution of activity in the safe and threat condition to the offset contrast, we selected active ROI voxels based on the data from the first run using a threshold of $p < .001$ uncorrected and plotted mean signal change in these voxels for each condition based on the data from Runs 2 and 3 to prevent overestimation of the effect size (41). Finally, we undertook an exploratory connectivity analysis to investigate the relationship between the activations in our ROIs. For this, we extracted the time course of activation in the ventromedial (vm)PFC ROI, calculated an interaction term for this time course and the contrast of interest, and added both the time course and the psychophysiologic interaction (PPI) term to our regression model adjusted for general effects of the task (42,43).

Results

Subjective Ratings

During both the MRI and startle session, subjects retrospectively reported more anxiety after the threat than after the safe cue [MRI $F(1,25) = 83.1$, $p < .001$; startle $F(1,22) = 74.3$, $p < .001$] and this difference was reduced significantly after cue offset [MRI $F(1,25) = 21.0$, $p < .001$; startle $F(1,22) = 38.7$, $p < .001$; see Table S1 in Supplement 1 for mean ratings per session]. For subjects that participated in both sessions, there was no difference in anxiety reported during the fMRI session and anxiety during the startle session [$Fs(1,22) < 1$, ns].

Startle Data

After threat onset, startle was increased compared with the safe condition [$F(1,25) = 40.5$, $p < .001$]. Fear-potentiated startle (FPS,

the difference in startle magnitude between threat and safe) fluctuated significantly across time points [threat condition × latency: $F(3,75) = 21.9, p < .001$], reflecting a reduction of startle magnitude to levels of the safe stimulus early after threat offset (see Figure 1). Repeated contrasts indicated that there was no difference in startle potentiation for probes presented early and late after cue onset [early cue vs. late cue: $F(1,25) = 2.4$, $p = .13$]. After threat offset, potentiation was quickly reduced [late cue vs. early offset: $F(1,25) = 46.2$, $p < .001$] and then stable again [early offset vs. late offset: $F(1,25) > 1$, ns]. Finally, the startle results were not influenced by previous experience with the task [order × threat condition and order × threat condition × time, Fs < 2.3, ns].

Imaging Data

Group Analyses

The group analysis focusing on brain areas that responded more during the threat cues than during the safe cues yielded activation in limbic areas. The active areas included the anterior insula/inferior frontal gyrus (IFG, BA 13/47 bilateral) and the dorsal ACC (BA 24/32; Figure 2, Table 1 for the whole brain group results). There was no activation in the amygdalae, also not when applying alternative analyses and thresholds (see Supplement 1). The critical contrast that compared threat offset to the offset of the safe condition indicated a significantly increased response in the right anterior lateral PFC (lPFC; BA 46/10, Figure 3, Table 1) to threat offset. In addition, there was a significant decrease in BOLD signal in the subgenual vmPFC after the offset of threat (BA 11, Figure 3, Table 1). Additional analyses involving the alternative contrast threat versus threat offset indicated that these prefrontal areas also responded more to threat offset than to the threat condition (see Figure 4; see Supplement 1 for the full results of these analyses).

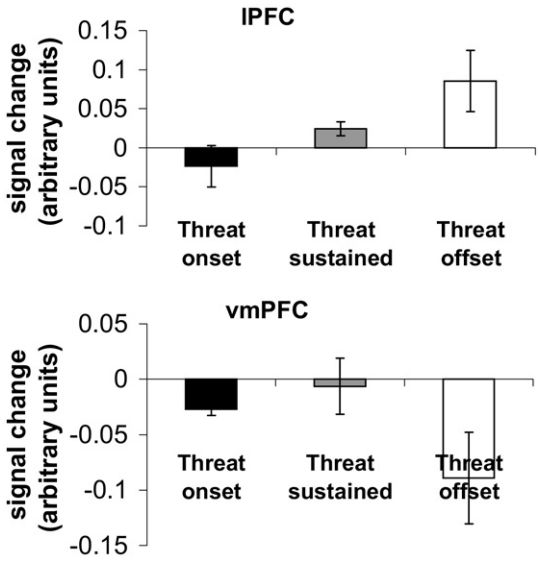

Figure 4. Percent signal change for each prefrontal region of interest for the threat onset, sustained, and threat offset conditions separately. These are again corrected for potential overestimation by using only the data from the last two runs from the region of interest that was determined based on the first run; the uncorrected data showed a similar pattern with stronger differentiation between the offset and the threat responses. Error bars represent standard error of the mean. lPFC, lateral prefrontal cortex; vmPFC, ventromedial prefrontal cortex.

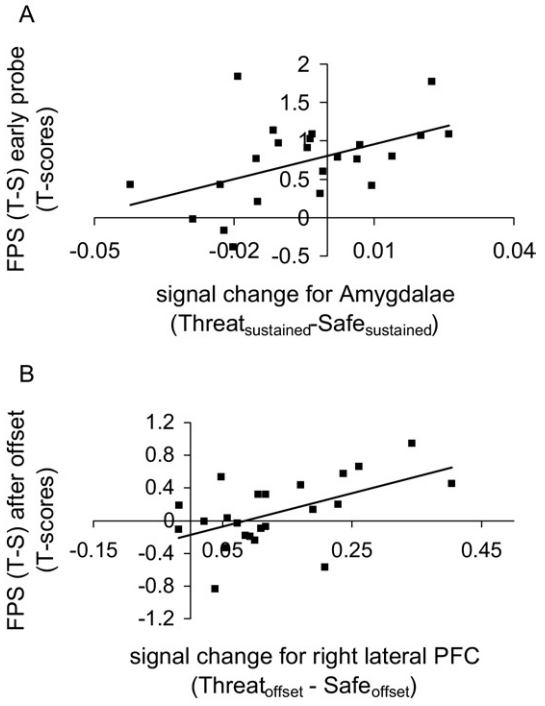

Figure 5. Correlations in signal change between functional magnetic resonance imaging data and the startle data. **(A)** Scatterplot of early startle potentiation (1.5–3.5 sec after onset) during the threat cue and differential blood oxygen level–dependent signal change in the amygdalae during threat. **(B)** Scatterplot of residual mean startle potentiation after threat offset and differential blood oxygen level–dependent signal change in the right lateral prefrontal cortex (PFC) to threat offset. FPS, fear-potentiated startle.

Between Subject Correlations

Next, we tested whether individual differences in FPS were associated with 1) recruitment of limbic regions of interest (insula, ACC, and amygdala) during threat and 2) recruitment of prefrontal ROIs (right lateral PFC and vmPFC) after threat offset. FPS during cue presentation, averaged across early and late probes, showed a marginally significant correlation with activation of the amygdalae during the fMRI session ($r = .38$, $p = .07$; see Figure 5a). This effect was most pronounced for the early probes for which the effect reached significance ($r = .47$, $p = .02$ for the early probe condition; $r = .17$, ns for late probes). Those subjects with a higher startle potentiation showed more amygdala activation to the threat vs. safe stimulus. No correlations were observed for the functional ROIs that showed increased activity to threat (insula, ACC), and there were also no correlations between FPS after offset and vmPFC activity after offset. However, those subjects with greater mean startle potentiation after the offset of the threat versus safe cue (early and late probes averaged) showed more mean activation in the right lPFC ROI after threat versus safe offset ($r = .54$, $p < .01$; see Figure 5b). This effect was significant for the late probes after threat offset ($r = .52$, $p < .01$) but not for the early probes ($r = .32$, ns).

Functional Connectivity

Finally, we investigated the hypothesis that the lPFC modulated limbic activity through the vmPFC. To this end, we examined correlations between activity in the right lateral prefrontal ROI and the subgenual vmPFC and also between the activity in the vmPFC and our limbic ROIs. This connectivity analysis showed a negative correlation between activity in the subgenual vmPFC and activity in a

region that overlapped with the right lPFC region activating in response to threat offset (again, all analyses $p < .001$ and family-wise error corrected at the cluster level $p < .05$). Moreover, there was also a negative correlation between vmPFC activity and activity in a right anterior limbic region encompassing the amygdala, anterior insula, and ventral striatum (Figure S1, Table S2 in Supplement 1). This indicates that stronger deactivations in the vmPFC co-occurred with more lPFC activity and more activity in these limbic regions. These correlations were based on the entire fMRI time courses recorded during the task. We found no evidence of a psychophysiologic interaction in response to threat offset, that is, we found no indications of significant changes in the correlations in response to the offset of the threat condition compared with the safe condition.

Discussion

The instructed fear paradigm increased both subjective anxiety and startle potentiation under conditions of threat. More important, the startle data also indicated that this fear response was quickly reduced to baseline levels across subjects within 3.5 sec. Together with previous research (17,22,44,45), this suggests that healthy subjects are able to adjust their defensive states rapidly in response to instructed conditions of threat and safety. Data from the fMRI session showed an increase in BOLD in the anterior insulae and dorsal ACC during the threat condition. These areas have been implicated in human anticipatory anxiety in many previous reports (33–38,46), and patients with anxiety disorders show hyperactivation in this circuit (1), suggesting that these structures play a central role in human anxiety (47,48). Perhaps surprising but in line with previous reports, our group analyses did not reveal discriminative activity in the amygdala in response to threat of shock (33,34,36,49). The amygdala response to threat may have habituated quickly while the defensive state remained (36,50,51). Our data do indicate that amygdala activations are found more consistently in subjects with higher startle potentiation early after threat onset. This is in line with animal work that has suggested a direct role for the amygdala in fear potentiation of the startle reflex (recently reviewed by Davis *et al.*) (3).

After offset of threat, the reduction in subjects' defensive state was accompanied by activity in the anterior part of the right lPFC. Lateral PFC activation has repeatedly been found to be associated with cognitive regulation of fear (5,11–13,16). These studies use more explicit regulation instructions, for example, to reappraise negative stimuli or feelings and find activations typically more dorsal than the area we found in this study (although see Phan *et al.*) (13). This could be due to higher demands in working memory in explicit regulation paradigms. Moreover, the finding that the activation at offset of the lPFC correlates positively with residual fear potentiation of the startle reflex after offset of the threat seems to indicate that the activation in this area does not automatically result in successful fear downregulation. Interestingly, Eippert *et al.* (11) also reported an inverse relation between emotion regulation success and activity in a slightly more posterior right lateral prefrontal region. We speculate that activation in this area may reflect effort to downregulate, which logically would be higher in subjects who have difficulty controlling fear, although this post hoc interpretation clearly requires further study.

Besides lPFC activity, we found a deactivation in the subgenual vmPFC after threat offset. The vmPFC is also frequently reported as part of the default mode network (52), signifying the potential importance of this area in returning the body to a homeostatic state. Studies on human fear extinction have also consistently reported involvement of the ventromedial PFC (9,10,53–55). The location of subgenual vmPFC activity in these studies corresponds well to the location of the deactivation observed at threat offset in our study, although these studies reported activation upon extinction relative to the prior fear state, rather than deactivation. With respect to this apparent controversy, it is interesting that in animals, deactivations of the vmPFC have been repeatedly linked to reductions in the expression of fear and stress (56–58), indicating that vmPFC activity is required for fear expression. However, vmPFC activity also appears required for reduction of fear through extinction (8,59). In humans, changes in vmPFC activity may also either promote or reduce fear, perhaps dependent on the state of the fear-promoting regions (58) and the specific anatomic pathway involved (8,56,57).

Because lPFC areas do not have strong direct connections to limbic areas such as the amygdala (60,61), the lPFC may control limbic activity that drives the fear response indirectly through the vmPFC (16). The results from our exploratory connectivity analyses support this idea by indicating that the lPFC and subgenual vmPFC interacted during our task. Although we found no direct evidence that this interaction became more pronounced around threat offset, the regions involved in this interaction matched the regions responding to threat offset well. Activity in the lPFC, matching the area activated after threat offset, was correlated with decreased activity in the subgenual vmPFC seed region. Moreover, deactivations in this vmPFC region were related to activity increases in the right lateral amygdala and anterior insula. On the basis of these exploratory analyses, we hypothesize that the latter increases may reflect activity in local limbic inhibitory circuits that control the output of the limbic system areas that instantiate anxiety. Perhaps, deactivations in the subgenual vmPFC may thus reduce activity in limbic output centers by activating inhibitory circuits located nearby (62). In line with this idea and our results, animal work has indicated that the vmPFC modulates amygdala output through recruitment of an inhibitory circuit based in lateral areas of the amygdala (59,63). Clearly, it is necessary to confirm the results from our exploratory analyses and further investigate the connectivity between the neural components involved in fear offset.

In conclusion, our new approach to investigate brain mechanisms involved in fear reduction at threat offset indicates overlap with mechanisms recruited in extinction and cognitive regulation of fear. We found that healthy subjects can flexibly downregulate their defensive states within a few seconds while recruiting ventromedial and right lateral prefrontal areas. Moreover, our results provide support for the idea that these prefrontal areas form a circuit that interacts with the limbic system in fear regulation in healthy humans. Together with previous research, this suggests that these areas in the PFC are broadly involved in fear control, and effective recruitment of these areas may be instrumental in protecting individuals from chronic forms of anxiety.

This project was partly funded by a Veni grant awarded to JMPB by the Netherlands organization for scientific research.

All authors report no biomedical financial interests or potential conflicts of interest.

Supplementary material cited in this article is available online.

1. Etkin A, Wager TD (2007): Functional neuroimaging of anxiety: A meta-analysis of emotional processing in PTSD, social anxiety disorder, and specific phobia. *Am J Psychiatry* 164:1476–1488.
2. Shin LM, Liberzon I (2009): The neurocircuitry of fear, stress, and anxiety disorders. *Neuropsychopharmacology*.

3. Davis M, Walker DL, Miles L, Grillon C (2010): Phasic vs sustained fear in rats and humans: Role of the extended amygdala in fear vs anxiety. *Neuropsychopharmacology* 35:105–135.
4. Grillon C, Lissek S, Rabin S, McDowell D, Dvir S, Pine DS (2008): Increased anxiety during anticipation of unpredictable but not predictable aversive stimuli as a psychophysiologic marker of panic disorder. *Am J Psychiatry* 165:898–904.
5. Ochsner KN, Gross JJ (2005): The cognitive control of emotion. *Trends Cogn Sci* 9:242–249.
6. Ochsner KN, Gross JJ (2008): Cognitive emotion regulation: Insights from social cognitive and affective neuroscience. *Curr Directions Psychol Sci* 17:153–158.
7. Hartley CA, Phelps EA (2010): Changing fear: The neurocircuitry of emotion regulation. *Neuropsychopharmacology* 35:136–146.
8. Quirk GJ, Beer JS (2006): Prefrontal involvement in the regulation of emotion: Convergence of rat and human studies. *Curr Opin Neurobiol* 16:723–727.
9. Gottfried JA, Dolan RJ (2004): Human orbitofrontal cortex mediates extinction learning while accessing conditioned representations of value. *Nat Neurosci* 7:1144–1152.
10. Phelps EA, Delgado MR, Nearing KI, LeDoux JE (2004): Extinction learning in humans: Role of the amygdala and vmPFC. *Neuron* 43:897–905.
11. Eippert F, Veit R, Weiskopf N, Erb M, Birbaumer N, Anders S (2007): Regulation of emotional responses elicited by threat-related stimuli. *Hum Brain Mapp* 28:409–423.
12. Ochsner KN, Bunge SA, Gross JJ, Gabrieli JD (2002): Rethinking feelings: An FMRI study of the cognitive regulation of emotion. *J Cogn Neurosci* 14:1215–1229.
13. Phan KL, Fitzgerald DA, Nathan PJ, Moore GJ, Uhde TW, Tancer ME (2005): Neural substrates for voluntary suppression of negative affect: A functional magnetic resonance imaging study. *Biol Psychiatry* 57:210–219.
14. Barbas H, Saha S, Rempel-Clower N, Ghashghaei T (2003): Serial pathways from primate prefrontal cortex to autonomic areas may influence emotional expression. *BMC Neurosci* 4:25.
15. McDonald AJ (1998): Cortical pathways to the mammalian amygdala. *Prog Neurobiol* 55:257–332.
16. Delgado MR, Nearing KI, Ledoux JE, Phelps EA (2008): Neural circuitry underlying the regulation of conditioned fear and its relation to extinction. *Neuron* 59:829–838.
17. Bocker KB, Baas JM, Kenemans JL, Verbaten MN (2004): Differences in startle modulation during instructed threat and selective attention. *Biol Psychol* 67:343–358.
18. Grillon C, Baas J (2003): A review of the modulation of the startle reflex by affective states and its application in psychiatry. *Clin Neurophysiol* 114:1557–1579.
19. Bradley MM, Moulder B, Lang PJ (2005): When good things go bad: The reflex physiology of defense. *Psychol Sci* 16:468–473.
20. Dichter GS, Tomarken AJ, Baucom BR (2002): Startle modulation before, during and after exposure to emotional stimuli. *Int J Psychophysiol* 43:191–196.
21. Germans GMG, Kring AM (2007): Sex differences in the time course of emotion. *Emotion* 7:429–437.
22. Grillon C, Ameli R, Merikangas K, Woods SW, Davis M (1993): Measuring the time course of anticipatory anxiety using the fear-potentiated startle reflex. *Psychophysiology* 30:340–346.
23. Jackson DC, Mueller CJ, Dolski I, Dalton KM, Nitschke JB, Urry HL, *et al.* (2003): Now you feel it, now you don't: Frontal brain electrical asymmetry and individual differences in emotion regulation. *Psychol Sci* 14:612–617.
24. Larson CL, Ruffalo D, Nietert JY, Davidson RJ (2005): Stability of emotion-modulated startle during short and long picture presentation. *Psychophysiology* 42:604–610.
25. Larson CL, Taubitz LE, Robinson JS (2010): MAOA T941G polymorphism and the time course of emotional recovery following unpleasant pictures. *Psychophysiology* 47, Nos. :857–62.
26. Klumpers F, van Gerven JM, Prinssen EP, Roche IN, Roesch F, Riedel WJ, *et al.* (2010): Method development studies for repeatedly measuring anxiolytic drug effects in healthy humans. *J Psychopharmacol* 24:657–666.
27. Neggers SF, Hermans EJ, Ramsey NF (2008): Enhanced sensitivity with fast three-dimensional blood-oxygen-level-dependent functional MRI: Comparison of SENSE-PRESTO and 2D-EPI at 3 T. *NMR Biomed* 21:663–676.
28. Ramsey NF, van den Brink JS, van Muiswinkel AM, Folkers PJ, Moonen CT, Jansma JM, Kahn RS (1998): Phase navigator correction in 3D fMRI improves detection of brain activation: Quantitative assessment with a graded motor activation procedure. *Neuroimage* 8:240–248.
29. Pruessmann KP, Weiger M, Scheidegger MB, Boesiger P (1999): SENSE: Sensitivity encoding for fast MRI. *Magn Reson Med* 42:952–962.
30. van Gelderen P, Ramsey NF, Liu G, Duyn JH, Frank JA, Weinberger DR, Moonen CT (1995): Three-dimensional functional magnetic resonance imaging of human brain on a clinical. 1.5-T scanner. *Proc Natl Acad Sci U S A* 92:6906–6910.
31. Blumenthal TD, Cuthbert BN, Filion DL, Hackley S, Lipp OV, van Boxtel A (2005): Committee report: Guidelines for human startle eyeblink electromyographic studies. *Psychophysiology* 42:1–15.
32. van Boxtel A, Boelhouwer AJ, Bos AR (1998): Optimal EMG signal bandwidth and interelectrode distance for the recording of acoustic, electrocutaneous, and photic blink reflexes. *Psychophysiology* 35:690–697.
33. Chua P, Krams M, Toni I, Passingham R, Dolan R (1999): A functional anatomy of anticipatory anxiety. *Neuroimage* 9:563–571.
34. Kumari V. (2007): ffytche DH; Das M, Wilson GD, Goswami S, Sharma T (2007): Neuroticism and brain responses to anticipatory fear. *Behav Neurosci* 121:643–652.
35. Nitschke JB, Sarinopoulos I, Mackiewicz KL, Schaefer HS, Davidson RJ (2006): Functional neuroanatomy of aversion and its anticipation. *Neuroimage* 29:106–116.
36. Phelps EA, O'Connor KJ, Gatenby JC, Gore JC, Grillon C, Davis M (2001): Activation of the left amygdala to a cognitive representation of fear. *Nat Neurosci* 4:437–441.
37. Seeley WW, Menon V, Schatzberg AF, Keller J, Glover GH, Kenna H, *et al.* (2007): Dissociable intrinsic connectivity networks for salience processing and executive control. *J Neurosci* 27:2349–2356.
38. Simmons A, Strigo I, Matthews SC, Paulus MP, Stein MB (2006): Anticipation of aversive visual stimuli is associated with increased insula activation in anxiety-prone subjects. *Biol Psychiatry* 60:402–409.
39. Brett M, Anton J, Valabregue R, Poline J (2002): Region of interest analysis using an SPM toolbox [Abstract]. Proceedings of the 8th International Conference on Functional Mapping of the Human Brain. *Neuroimage* 16:abstract 497.
40. Tzourio-Mazoyer N, Landeau B, Papathanassiou D, Crivello F, Etard O, Delcroix N, *et al.* (2002): Automated anatomical labeling of activations in SPM using a macroscopic anatomical parcellation of the MNI MRI single-subject brain. *Neuroimage* 15:273–289.
41. Kriegeskorte N, Simmons WK, Bellgowan PS, Baker CI (2009): Circular analysis in systems neuroscience: The dangers of double dipping. *Nat Neurosci* 12:535–540.
42. Friston KJ, Buechel C, Fink GR, Morris J, Rolls E, Dolan RJ (1997): Psychophysiological and modulatory interactions in neuroimaging. *Neuroimage* 6:218–229.
43. Gitelman DR, Penny WD, Ashburner J, Friston KJ (2003): Modeling regional and psychophysiologic interactions in fMRI: the importance of hemodynamic deconvolution. *Neuroimage* 19:200–207.
44. Baas JM, Grillon C, Bocker KB, Brack AA, Morgan CA 3rd, Kenemans JL, Verbaten MN (2002): Benzodiazepines have no effect on fear-potentiated startle in humans. *Psychopharmacology* 161:233–247.
45. Mol N, Baas JM, Grillon C, van Ooijen L, Kenemans JL (2007): Startle potentiation in rapidly alternating conditions of high and low predictability of threat. *Biol Psychol* 76:43–51.
46. Straube T, Mentzel HJ, Miltner WH (2007): Waiting for spiders: Brain activation during anticipatory anxiety in spider phobics. *Neuroimage* 37:1427–1436.
47. Milad MR, Quirk GJ, Pitman RK, Orr SP, Fischl B, Rauch SL (2007): A role for the human dorsal anterior cingulate cortex in fear expression. *Biol Psychiatry* 62:1191–1194.
48. Paulus MP, Stein MB (2006): An insular view of anxiety. *Biol Psychiatry* 60:383–387.
49. Mechias ML, Etkin A, Kalisch R (2010): A meta-analysis of instructed fear studies: Implications for conscious appraisal of threat. *Neuroimage* 49:1760–1768.
50. Marschner A, Kalisch R, Vervliet B, Vansteenwegen D, Buchel C (2008): Dissociable roles for the hippocampus and the amygdala in human cued versus context fear conditioning. *J Neurosci* 28:9030–9036.
51. Zald DH (2003): The human amygdala and the emotional evaluation of sensory stimuli. *Brain Res Brain Res Rev* 41:88–123.

52. Gusnard DA, Raichle ME (2001): Searching for a baseline: Functional imaging and the resting human brain. *Nat Rev Neurosci* 2:685–694.
53. Milad MR, Quinn BT, Pitman RK, Orr SP, Fischl B, Rauch SL (2005): Thickness of ventromedial prefrontal cortex in humans is correlated with extinction memory. *Proc Natl Acad Sci U S A* 102:10706–10711.
54. Kalisch R, Korenfeld E, Stephan KE, Weiskopf N, Seymour B, Dolan RJ (2006): Context-dependent human extinction memory is mediated by a ventromedial prefrontal and hippocampal network. *J Neurosci* 26:9503–9511.
55. Milad MR, Wright CI, Orr SP, Pitman RK, Quirk GJ, Rauch SL (2007): Recall of fear extinction in humans activates the ventromedial prefrontal cortex and hippocampus in concert. *Biol Psychiatry* 62:446–454.
56. Radley JJ, Arias CM, Sawchenko PE (2006): Regional differentiation of the medial prefrontal cortex in regulating adaptive responses to acute emotional stress. *J Neurosci* 26:12967–12976.
57. Sierra-Mercado D Jr, Corcoran KA, Lebron-Milad K, Quirk GJ (2006): Inactivation of the ventromedial prefrontal cortex reduces expression of conditioned fear and impairs subsequent recall of extinction. *Eur J Neurosci* 24:1751–1758.
58. Sullivan RM (2004): Hemispheric asymmetry in stress processing in rat prefrontal cortex and the role of mesocortical dopamine. *Stress* 7:131–143.
59. Sotres-Bayon F, Bush DE, LeDoux JE (2004): Emotional perseveration: An update on prefrontal-amygdala interactions in fear extinction. *Learn Mem* 11:525–535.
60. Ghashghaei HT, Barbas H (2002): Pathways for emotion: Interactions of prefrontal and anterior temporal pathways in the amygdala of the rhesus monkey. *Neuroscience* 115:1261–1279.
61. Ghashghaei HT, Hilgetag CC, Barbas H (2007): Sequence of information processing for emotions based on the anatomic dialogue between prefrontal cortex and amygdala. *Neuroimage* 34:905–923.
62. Herman JP, Ostrander MM, Mueller NK, Figueiredo H (2005): Limbic system mechanisms of stress regulation: Hypothalamo-pituitary-adrenocortical axis. *Prog Neuropsychopharmacol Biol Psychiatry* 29:1201–1213.
63. Rosenkranz JA, Moore H, Grace AA (2003): The prefrontal cortex regulates lateral amygdala neuronal plasticity and responses to previously conditioned stimuli. *J Neurosci* 23:11054–11064.